

Wave Hindcasting Using WAM and WAVEWATCH III: A Comparison Study Utilizing Oceansat-2 (OSCAT) Winds

Swain J¹, Umesh PA^{1,3*}, Balchand AN² and B. Prasad Kumar³

¹Naval Physical and Oceanographic Laboratory, Kochi-21, India

²Department of Physical Oceanography, Cochin University of Science and Technology, Kochi-16, India

³Department of Ocean Engineering and Naval Architecture, Indian Institute of Technology Kharagpur, Kharagpur-02, India

Abstract

In this study, the state-of-the-art third generation wave models WAM and WAVEWATCH-III (WWIII) have been used to predict waves for the North Indian Ocean over $1^\circ \times 1^\circ$ (lat \times long) grid resolutions utilizing six-hourly processed winds which was possible with the launch of OCEANSAT-2 (OSCAT) by ISRO, on 23 September 2009. The study demonstrates the application of interpolated OSCAT winds to hindcast waves across the globe using two deep-water models WAM and WAVEWATCH III (WWIII) and to compare the skill of the models using error analysis. In this context, the wave models WAM and WWIII were forced using OSCAT winds for the year 2011 over the global domain as well as for the North Indian Ocean (regional domain) using appropriate boundary conditions/inputs. The output from the models such as significant wave height (Hs) and mean wave period (Tc) were validated with an NDBC buoy measurement during January to December 2011 in the North Atlantic Ocean and for few selected buoys in the Bay of Bengal for the month of July 2011 (peak southwest monsoon). The comparisons of OSCAT winds with NDBC wind measurements reveal that the overall trend and dominant directions are consistent with the observational data. The validation of significant wave parameters of the selected buoy in the North Atlantic ocean revealed very high correlation ($R > 0.9$) with percentage error $< 20\%$ for Hs and Tc. The comparisons between the observed and predicted wave parameters in the Bay of Bengal showed that percentage error ranged between 9 to 24% for Hs and within 10% for Tc. It is noted that WAM describes the variability of wave heights realistically with smaller error estimates and better correlation coefficients than WWIII. Such validation studies are proven to be useful in quantifying the performance of these wave models which are being utilized or yet to be further explored for routine operational applications as well as for long-term wave hindcasting in the strategic areas of importance in deep as well as shallow waters by nesting with suitable near-shore models in the littoral zone.

Keywords: WAM; WWIII; Sea-state prediction; OSCAT winds; Wave model validation

Introduction

Information on ocean surface waves which is often referred to as the 'sea-state' is most essential for naval operation/warfare, offshore operations, rescue operations, ship routing (OTSR-Optimum Tracking of Ship Routes), design/development of harbors, coastal protection/engineering, wave climate assessment, recreation etc. During the last twenty years or so, the third generation wave model WAM, Cycle-4 [1] has become a standard for routine operational wave prediction purpose, besides the ongoing research and engineering applications. The quality of wave prediction and analysis is also being continuously improved mainly due to the availability of high quality input wind fields for sea-state prediction with the advancement of satellite measurements/oceanography. In the Indian context, there are many reported important research contributions on wave prediction/hindcasting using third generation wave models [2-9].

In this study, the state-of-the-art third generation wave models such as WAM and WWIII (WAM: Cycle-4.5.3, and WAVEWATCH-III [10]: WWIII V3.14) have been implemented for the globe over $1^\circ \times 1^\circ$ resolution (deep water) for wave hindcasting using OSCAT winds. Although, since the launch of OCEANSAT II, wind analysis studies using OSCAT winds are reported, there are no studies available for wave hindcasting in the North Indian Ocean using OSCAT wind inputs. In the context wherein wave models require analysed wind fields as input, and input winds are the determining driving forces for realistic wave model outputs, the study is unique and of its first kind reporting the application of interpolated scatterometer winds to hindcast waves over the globe using two deep-water models WAM and WWIII. The study aims to demonstrate the utility of Oceansat-2 winds for the simulation or prediction of wave parameters in the North Indian

Ocean and comparison of two wave models in the simulation of wave characteristics. The output from these models such as significant wave height and mean wave period are validated with buoy measurements in the global oceans and in the Bay of Bengal and further the skill of these models is assessed with an extensive statistical error analysis.

Wave Models: WAM and WWIII

The WAM, a third-generation wave prediction model solves the following spectral energy balance equation for describing the two-dimensional wave spectrum:

$$\frac{\partial F}{\partial t} + \nabla \cdot (C_g F) = S_{in} + S_{nl} + S_{ds} \quad (1)$$

where $F(f, \bar{\theta}; \bar{x}, t)$ is the spectral wave energy density; depending on wave frequency (f), wave direction (θ), position (\bar{x}), and time (t) and deep-water group velocity $C_g = C_g(f, \theta)$. The source functions, on the right hand side of Equation 1, describe the wind input (S_{in}), nonlinear transfer (S_{nl}), and dissipation due to white-capping (S_{ds}).

***Corresponding author:** Umesh PA, Department of Ocean Engineering & Naval Architecture, Indian Institute of Technology Kharagpur, Kharagpur, West Bengal India, Tel: +91-3222-255221 and Fax: +91-3222-255303; E-mail: umeshpa.nair@gmail.com, umesh@naval.iitkgp.ernet.in

Received August 04, 2017; Accepted August 30, 2017; Published September 07, 2017

Citation: Swain J, Umesh PA, Balchand AN, Kumar BP (2017) Wave Hindcasting Using WAM and WAVEWATCH III: A Comparison Study Utilizing Oceansat-2 (OSCAT) Winds. J Oceanogr Mar Res 5: 166. doi: 10.4172/2572-3103.1000166

Copyright: © 2017 Swain J, et al. This is an open-access article distributed under the terms of the Creative Commons Attribution License, which permits unrestricted use, distribution, and reproduction in any medium, provided the original author and source are credited.

The WWIII is an extension of the WAM model developed and implemented at NOAA/NCEP [11]. The general source terms used in WWIII are defined as:

$$S = S_{in} + S_{nl} + S_{ds} + S_{bot} + S_{db} + S_{tr} + S_{sc} + S_{xx} \quad (2)$$

In deep waters, the net source term S is generally considered to consist of three parts, a wind-wave interaction term (S_{in}), a nonlinear wave-wave interactions term (S_{nl}) and a dissipation (whitecapping) term (S_{ds}). The input term (S_{in}) is dominated by the exponential growth term, and the source term generally describes this dominant process. To initialize the model and thereby to provide more realistic initial wave growth, a linear input term (S_{in}) is also considered in WWIII. In shallow waters, additional processes are notably wave-bottom interactions (S_{bot}). In near-shore waters, depth-induced breaking (S_{db}) and triad wave-wave interactions (S_{tr}) are considered important. The source/sink terms in WWIII also handles the scattering of waves by bottom features (S_{sc}) and slot for additional user defined source terms (S_{xx}).

Materials and Methods

Model set up and wave data

In this study, the recent versions of WAM (C4.5.3) [12] and WWIII (V3.14) are implemented for wave hindcasting over the global domain using OSCAT winds. The global grid system for WAM and WWIII covers the geographical extents 0° to 360° E and 77° S to 77° N with a resolution $1^\circ \times 1^\circ$ and the regional grid system extends from 50° to 100° E and 0° N to 30° N with the similar resolution. The WAM model uses 25 frequencies ranging from 0.04177 Hz to 0.41145 Hz and 12 directions (constant increment) to represent the wave spectra distribution. Similarly, the WWIII model uses 25 frequencies ranging from 0.0412 Hz to 0.4056 Hz, with a logarithmic distribution having an increment factor 1.1 and 24 directions (constant increment). Considering the observed data gaps of OSCAT winds, the models were first executed for the global domain. It takes care of southern ocean swell propagations and subsequently executed over the regional domain by taking the boundary inputs from the global run. This approach takes care of swells propagating from south and improved the model predictions, especially the combined sea and swell components in the region of interest by changing the model setting and integration time-steps appropriately as compared to the global run. The wave data utilized in this study is for a selected NDBC (NOAA Data Buoy Center) buoy, located (22.120° N, 93.960° W) in the North Atlantic Ocean (Buoy ID: 42055, Bay of Campeche) at a depth of 3595 m. The NDBC is a part of the National Oceanic and Atmospheric Administration's (NOAA) National Weather Service (NWS). NDBC designs, develops, operates, and maintains a network of data collecting buoys and coastal stations. Apart from NDBC buoy the study also used data from three selected NIOT buoy locations BD08 (off Paradip), BD11 (off Nellore) and BD14 (off Sri Lanka) at a depth of 2200 m, 3369 m and 3800 m respectively in the Bay of Bengal. The location of the buoys is as shown in Figure 1. The moored buoys (NIOT buoys) are floating platforms designed to carry specific suit of sensors to measure meteorological and oceanographic parameters.

Model inputs

In the present study, Level-2B (L2B) operational wind products (Version 1.3, October 2011) from OSCAT made available by National Remote Sensing Centre (www.nrsc.gov.in) was used to force the above mentioned wave models. OSCAT winds have been processed and analyzed for the period January to December 2011. Since there were data gaps (and missing data as well) and time gaps during the global coverage of OCEANSAT II, the gridded wind fields were prepared

through spatio-temporal interpolation of these winds [13] at six-hourly interval over $1^\circ \times 1^\circ$ resolution, which were provided as input to the wave models. The models were executed using these 6-hourly interpolated OSCAT winds. The model bathymetry was constructed from ETOPO2 data. The current data required as input for both wave models are obtained from the Ocean Surface Current Analyses-Real-time (OSCAR) database [14]. The ERA-interim daily fields from ECMWF were used to extract the air-sea temperature difference data as input for WWIII model.

Comparison of OSCAT winds with NDBC measurements

Before the OSCAT winds were used to simulate the waves over the globe, an attempt is made to compare the input winds for the year 2011 (January to December) using the NDBC buoy data. The comparison of OSCAT (wind speed and direction) and NDBC buoy data was executed for one location in the North Atlantic Ocean (Buoy ID: 42055, Bay of Campeche). For the validation purpose, OSCAT wind vectors were collocated with the buoy wind data both in space and time. The nearest four grids have been selected and the data is spatially interpolated following inverse distance approach to estimate wind speed and direction. Similarly the nearest interpolated/estimated values which correspond to the past and future time zones have been interpolated (temporal) linearly to estimate six hourly winds.

Prediction of deep water ocean surface waves using WAM

Wave hindcasts were carried out globally by using the six-hourly winds (and other inputs as indicated above) starting with five days prior to 1st January 2011, until end of the December 2011 (last day). Initially, the wave models were set to cold start and the five days computation prior to the selected month was sufficient to generate the initial fields for the start time of the month (first day of global run). WAM was subsequently executed for the regional grid using the same six-hourly winds from 1st July 2011, till end of the month by incorporating the initial conditions and boundary inputs from global run (warm start).

Prediction of deep water ocean surface waves using WWIII

Similar to WAM as explained above, WWIII was also executed for predicting waves globally (77.5° S, 77.5° N; 0.5° W, 359.5° E) for the year 2011 and regionally (Indian Seas, 50° to 100° E and 0° N to 30° N) over $1^\circ \times 1^\circ$ grid resolutions utilising the same OSCAT winds for the month of July 2011. In comparison with WAM, WWIII uses an additional input air-sea temperature difference apart from winds and currents.

Validation of WAM and WWIII models

Based on the availability of buoy data pertaining to the study period and the region of interest, comparisons were made between the buoy measurements and model derived wave heights and wave periods. The NDBC buoy located in the North Atlantic Ocean (Buoy ID: 42055) is used to validate the WAM/ WWIII global simulated wave parameters H_s and T_c . Apart from this, the in-situ met-ocean buoy parameters such as H_s and T_c of NIOT (disseminated by INCOIS, Hyderabad) for the buoys located in the Bay of Bengal (Figure 1) named BD08 (off Paradip), BD11 (off Nellore) and BD14 (off Sri Lanka) have been co-located with WAM and WWIII model outputs and interpolated in space and time for the comparisons/validations. A detailed statistical error analysis is performed for each dataset to evaluate the model performance. Various statistical measures such as Coefficient of Correlation (R), Scatter Index (SI), Bias (B, mean deviation), Root Mean Square Error (RMSE), Percentage Error (PE) and Model Performance Index (MPI) between measurements [15,16] and model outputs were computed and further examined to evaluate the performance of model hindcasts.

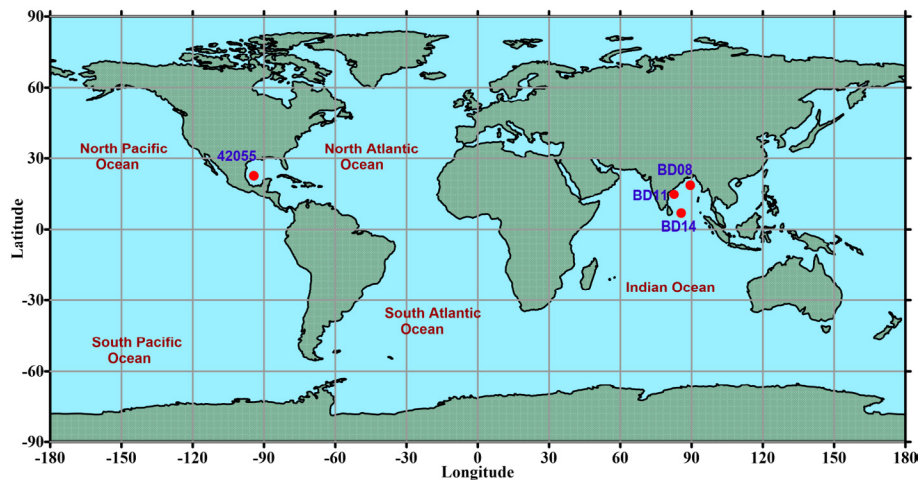


Figure 1: Location of moored buoys utilised for WAM and WWIII validations.

Results and Discussion

Comparison of OSCAT winds with NDBC measurements

The OSCAT wind speeds revealed good agreement with NDBC buoy measured wind speeds in the North Atlantic Ocean, as evident from the time series plot (Figure 2). It is clear from the time series plots (Figure 2) that the OSCAT winds do not have appreciable bias with respect to observations at buoy location. The statistics of the validation of wind speed is presented in Table 1. The average wind speed and standard deviations demonstrates almost the same range as buoy observations at the study area. However, it is noted from the standard deviations that the buoy wind speeds are more scattered in comparison with the OSCAT wind speeds. A high correlation coefficient of 0.98 and RMSE of 1.18 indicate a good match between buoy and OSCAT winds. The high correlation coefficients recommend that both measured and OSCAT winds follow a similar annual pattern. Similar to wind speed it is noted the wind directions also followed the trend and the leading directions are in good match with the measured data. The OSCAT mission requirements for the RMSE in wind speed is less than 2 m/s (for wind direction less than 20°) for the 4-24 m/s speed range. The statistics shown in Table 1 satisfies the mission requirements and hence compares well with the study by Kumar et al. [17].

Prediction of deep water ocean surface waves using WAM

The sample spatial plots (contours) of input wind fields as well as the corresponding output fields of significant wave height (Hs) for a selected day and time (spatial variability for 1200 hrs), i.e. for 25 July 2011 are shown in Figures 3 and 4a respectively (global domain). Figure 3 shows that the wind speed varied from 4 to 12 m/s in the North Indian Ocean on 25 July 2011 (1200 hrs). It is also seen that the wind speed and direction, which prevailed in the North Indian Ocean region on 25 July 2011 more or less, represents the standard climatological pattern of wind variability [18,19].

The wind and wave conditions in the Arabian Sea and Bay of Bengal (Indian Seas) are generally high during the southwest monsoon [18,19] that is considered as the roughest weather season from wave climate point of view. However, the wave periods and swell parameters are normally not related to the local winds as the waves propagate from different areas after their generation, which is evident from the sample

model outputs as shown in Figures 5 and 6. In the Arabian Sea, Hs varied from 1.0 to 3.0 m, while mean wave period (Tc) ranged from 7 to 10s. The swell wave height (Hsw) varied from 1.0 to 2.5 m while swell wave period (Tsw) varied from 9 to 10s. However, in the Bay of Bengal, Hs was relatively lower (1.0 to 2.5 m) as compared to the Arabian Sea. The Tc varied from 6 to 9s, Hsw from 0.5 to 1.5 m, and Tsw from 7 to 9s.

Prediction of deep water ocean surface waves using WWIII

The sample spatial plot (contours) of wave output field (Hs) for a selected day (25 July 2011, 1200 hrs) is shown in Figure 4b for the global domain. It is seen from this figure that, the spatial distribution of Hs and the mean wave directions (arrows) based on WAM and WWIII are well in good agreement with each other (25 July 2011, 1200 hrs). The areas of high wave activity also agree considerably well with each other.

The spatial variability of wave parameters as shown for 25 July 2011, 1200 hrs (Figures 5 and 6), is a typical example of high wave activity during the peak southwest monsoon period. As shown in Figure 6 (WWIII hindcast), the Hs varied from 1.0 to 3.5 m in the Arabian Sea, while in the Bay of Bengal it ranged between 1.0 to 1.5 m. The Tc varied from 5 to 9s in the Arabian Sea and from 5 to 7s in the Bay of Bengal. Similarly, the hindcasted Hsw varied from 1.0 to 3.0 m in the Arabian Sea, and in Bay of Bengal it varied from 0.5 to 1.5 m. In the Arabian Sea, the Tsw varied from 7 to 9s, while in the Bay of Bengal it ranged from 6 to 8s. The spatial variability of these significant wave parameters indicate that, there are certain differences in the magnitudes of the hindcast wave parameters between the two models using the same input wind fields. However, a quantitative inter-comparison can reveal the relative performances of both models that are discussed in the next section.

Validation of WAM and WWIII models

The model outputs analysed and discussed in the previous sections serves as the background information useful to validate the results using buoy data. To assess the model performance the simulated significant wave height and mean wave period are compared (Figure 7) with the NDBC buoy observations (42055) for the period January to December 2011. The comparisons shows that the WAM model derived wave parameters agree well with the observed wave parameters as shown in Figure 7. In the case of

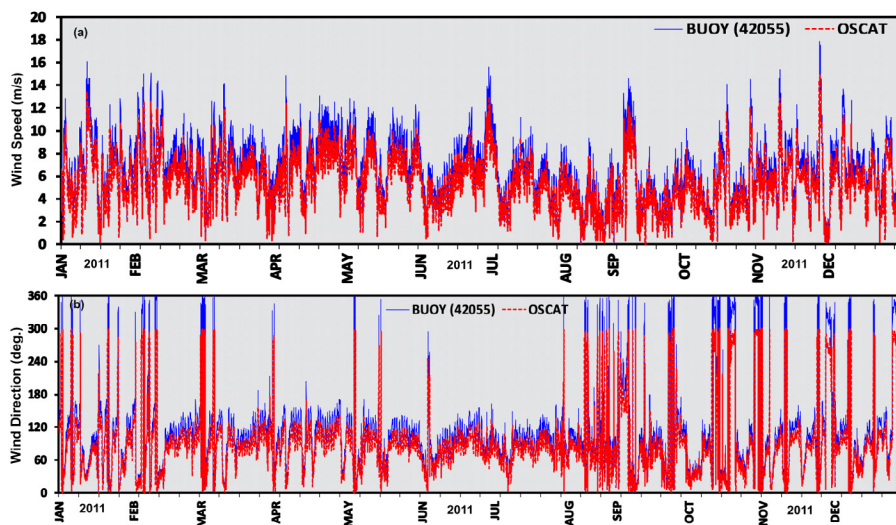


Figure 2: Time series plot of buoy and OSCAT (a) wind speed (m/s) and (b) wind direction (deg.) at NDBC (42055) buoy location.

Buoy location	Average (m/s)		Standard deviation (m/s)		Bias (m/s)	RMSE (m/s)	Correlation
	Buoy	OSCAT	Buoy	OSCAT			
NDBC (42055)	6.52	6.43	2.78	2.32	-0.19	1.18	0.98

Table 1: Comparison of OSCAT and buoy observations (January to December 2011).

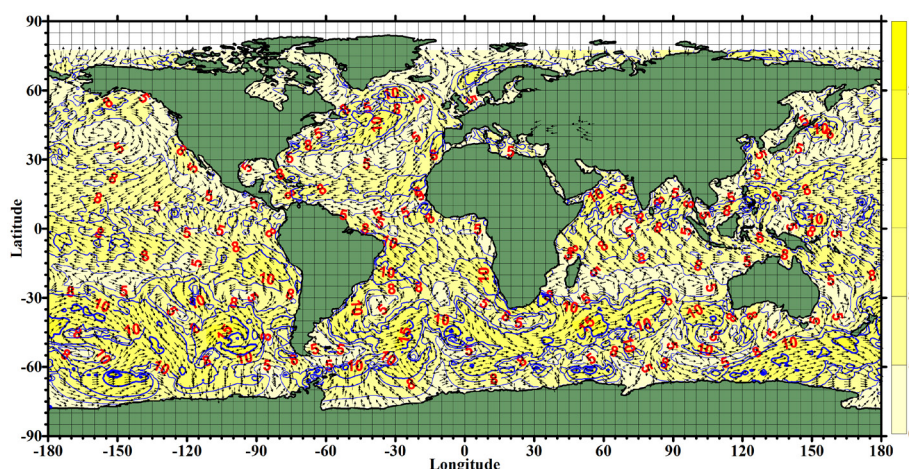


Figure 3: A sample input wind field (OSCAT), speed (m/s) and direction (arrows) for wave hindcasting using WAM (& WWIII), 25 July 2011, 1200 hrs.

Hs, the comparisons (Table 2) gave a strong correlation ($R=0.98$), with low SI (0.15) and RMSE (0.19). The negative bias denotes slight underestimation. Quantitatively, the model output obtained here are consistent with those obtained at the buoy location for the year 2011 with PE=15% and high MPI (0.92). It is observed that the model could reproduce the variability in wave heights at that buoy location. The overall trend in wave heights shows a reasonable good match with buoy observations. Similarly the comparison of Tc, also demonstrated strong correlations ($R=0.98$) with low SI and PE of 8.2% revealing a good match at the buoy location. The WWIII model simulated outputs when compared with the buoy measurements during January to December 2011 exhibited slightly lesser performances as compared with the WAM outputs. It is noted that similar to WAM slight underestimation by WWIII is also noted ($B= -0.12$) for Hs. Although it shows a strong correlation ($R= 0.97$),

the PE is 19.3% which is slightly higher in comparison with WAM. In case of Tc simulations by WWIII, significant underestimations were noted ($B= -0.18$) as compared with WAM. It is noted that the PE was higher 16.3% which denotes a higher disagreement in comparison with WAM Tc. In this buoy location in the North Atlantic (42055), it is observed that WAM generally follow the observations well and displays similar variability. WWIII on the other hand displays a much smoother wave height evolution, but it is able to capture the highest and lowest wave conditions with slightly higher errors than WAM. It is very encouraging to see that WAM is capable of capturing realistically both Hs and Tc in comparison with WWIII, which showed higher PE in simulating Hs and Tc at the buoy location. Although WWIII does not show clearly better behavior than WAM, for this location the systematically more realistic variability of wave heights produced by WWIII is evident in the comparison.

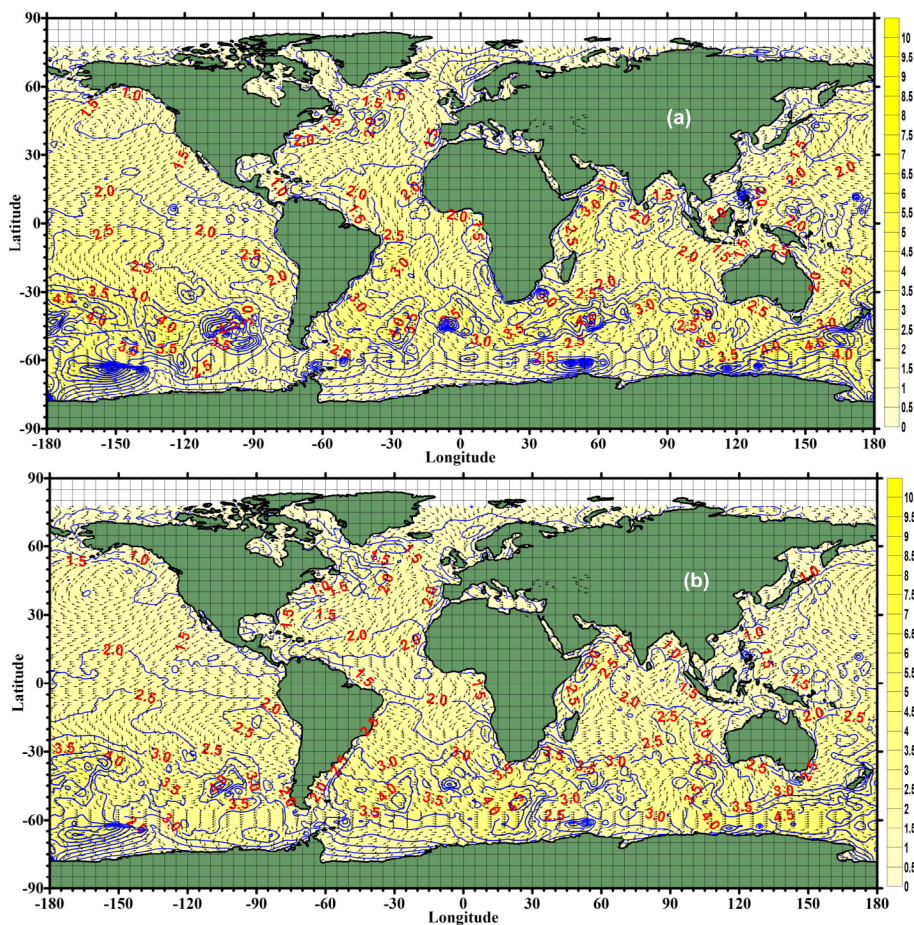


Figure 4: (a) WAM and (b) WWIII predicted significant wave height (m) & mean wave direction (arrows), 25 July 2011, 1200 hrs, and using OSCAT winds.

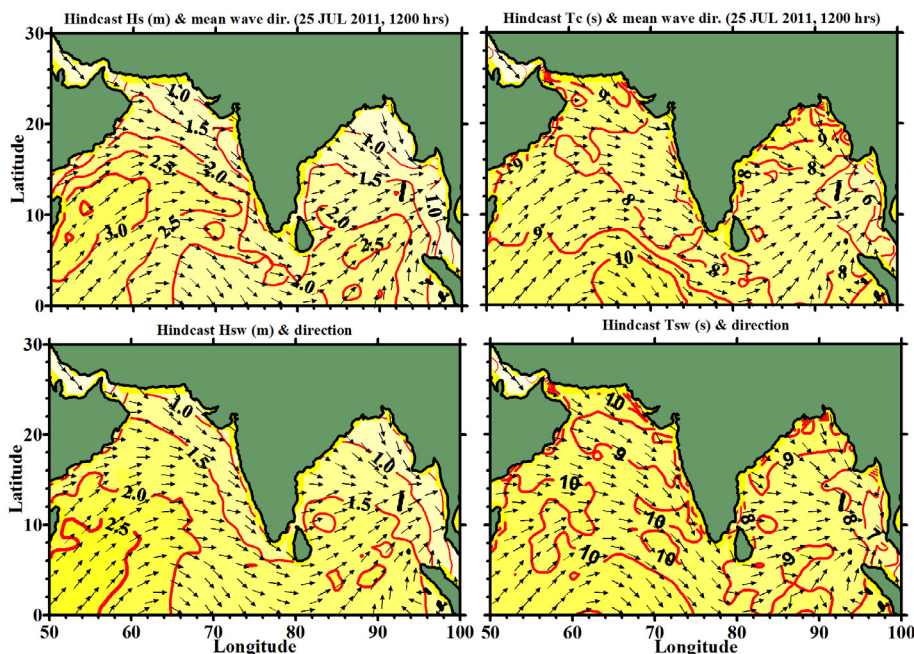


Figure 5: WAM hindcast wave fields (Hs, Tc, Hsw & Tsw) using OSCAT winds, 25 July 2011, 1200 hrs.

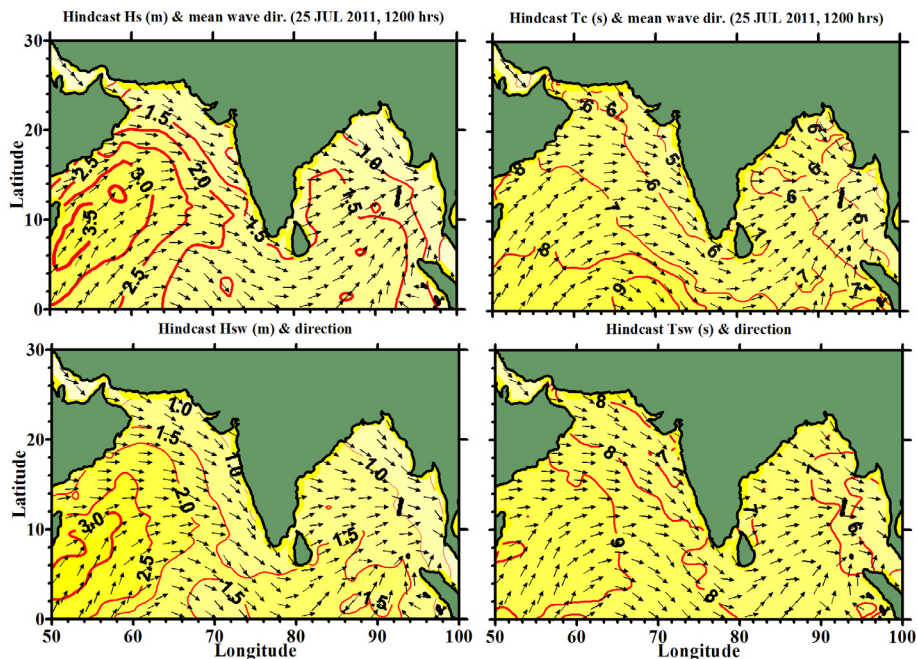


Figure 6: WWIII hindcast wave fields (Hs, Tc, Hsw & Tsw) using OSCAT winds, 25 July 2011, 1200 hrs.

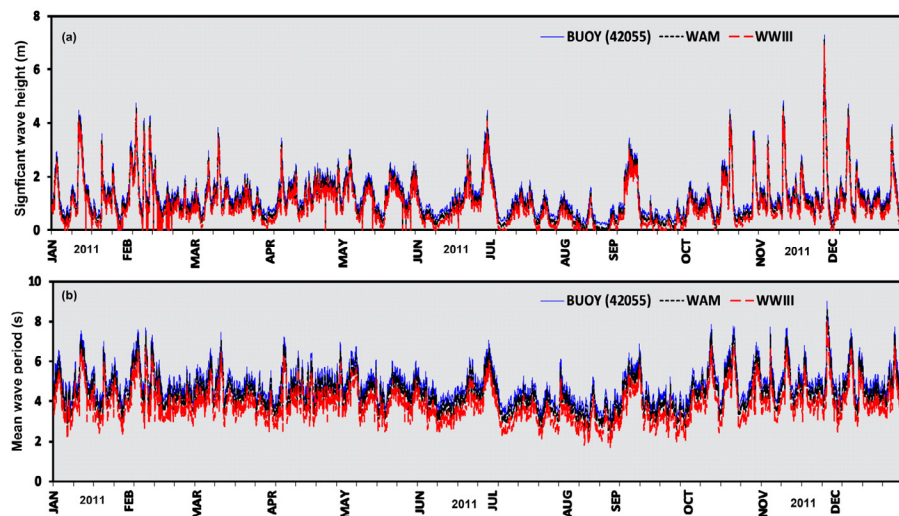


Figure 7: Time series plots of buoy and model simulated wave parameters at NDBC buoy location 42055, (a) Significant wave height (m) and (b) mean wave period (s).

As shown in Figure 8, WAM hindcasts (Hs and Tc) have been compared with three buoys (Bay of Bengal) such as BD08 (off Paradip), BD11 (off Nellore) and BD14 (off Sri Lanka) for the periods 01-15 July, 01-15 July, and 08-15 July 2011 respectively and their statistical estimates are shown in Table 3. It is seen that, the estimated R values for Hs are >0.9, with SI values of the order 0.01 to 0.10; and RMSE 0.03 m to 0.30 m, all indicating a good agreement between the model and buoy measurements during the active southwest monsoon winds of July 2011. The bias (Hs) is positive throughout for all buoys considered. The values of PE are in the range 8.5% to 20.2%. Although the MPI is >0.9 in all cases; it is noted that the buoy BD11 shows fairly a good agreement compared to BD14 and BD08. Compared to Hs, the Tc shows relatively lower correlation ($R > 0.7$) with low SI and RMSE of the order 0.10 to 0.23s; which indicate generally a better fit between the model and buoys.

Moreover, the computed values of bias are 0.41s (BD08), -0.05s (BD11) and 0.20s (BD14) that signify that, the WAM model predicts Tc well within an error of 0.5s. The PE values are low (<8%) at all the buoy locations in the Bay of Bengal. Values of MPI for Tc are >0.95 which indicates a good agreement between the WAM and buoy measurements.

Similarly, Figure 8 also shows the comparison between the observed and predicted wave parameters (Hs and Tc) of WWIII for the period 01-15 July 2011. In this case, the model outputs are validated for the same three buoy locations such as BD08 (off Paradip), BD11 (off Nellore) and BD14 (off Sri Lanka) located in the Bay of Bengal. The computed statistical estimates for the WWIII hindcast parameters (Hs and Tc) and the buoy measurements during July 2011 are also shown in Table 3. The WWIII hindcasts and the measurements of buoys BD08,

2.1. Significant wave height (Hs in m)		
WAM/WWIII		
S. No.	Statistical estimates	Atlantic Ocean (42055)
1	Mean (Buoy)	1.3
2	Range (Buoy)	0.1–7.3
3	Mean (WAM/WWIII)	1.11/0.91
4	Range (WAM/WWIII)	0.1–7.11/0.1–6.91
5	R	0.98/0.97
6	SI	0.15/0.30
7	B	-0.07/ -0.12
8	RMSE	0.19/0.31
9	PE	15.12/19.33
10	MPI	0.92/0.88
2.2. Mean wave period (Tc in s)		
WAM/WWIII		
1	Mean (Buoy)	4.84
2	Range (Buoy)	2.7–9.0
3	Mean (WAM/WWIII)	4.4/3.8
4	Range (WAM/WWIII)	2.3–8.6/1.7–8.0
5	R	0.98/0.93
6	SI	0.08/0.21
7	B	-0.04/ -0.18
8	RMSE	0.28/0.40
9	PE	8.2/16.3
10	MPI	0.96/0.85

R: Correlation Coefficient; SI: Scatter Index; B: Bias; RMSE: Root Mean Square Error; PE: Percentage Error; MPI: Model Performance Index

Table 2: The statistics of the comparison between buoy (NDBC) and simulated (WAM/WWIII) wave parameters Hs and Tc (January to December 2011).

BD11 and BD14 showed high correlation coefficients ($R > 0.9$) for Hs. The values of SI are lower indicating a better fit between the measured and model Hs. Positive bias is observed for all buoys considered which signifies that, model computed Hs are marginally higher compared to buoy observations. The RMSE varied from 0.03 to 0.38 m. It is noted that although the MPI is > 0.86 for all buoys considered, the PE for Hs is 9.1% for BD11, while it is considerably higher for BD08 (23.8%) and BD14 (24.1%) where the model could not predict Hs, well at these two buoy locations. Based on the present case study as well as the case studies earlier described, it is noticed that MPI alone does not appear to be a measure of the model performance/validation. Hence, it is appropriate to consider all the six statistical estimates together as shown in Table 3 (Sl. No. 5 to 10) for a proper assessment of model performance. The Tc also showed reasonably good correlation (Table 3) of 0.93 (R) for BD08, while it showed lower correlations of 0.68 for BD11 and 0.53 for BD14. SI is low with RMSE of the order 0.11s to 0.40s and Bias is negative for BD11 (-0.04s), BD14 (-0.07s) and positive in the case of BD08 (0.59s). The PE remained within 10% for all buoys with $MPI > 0.9$ which showed a reasonably good agreement between model and buoy observations.

Overall, the comparison of WAM and WWIII hindcasts shows low SI, smaller RMSE with very low PE, as well as a better correlation coefficient for WAM. However, WWIII has higher estimates of SI, RMSE and PE; and in general is lesser energetic against buoy data. The time series plots as shown in Figures 7 and 8 and the statistics shown in Tables 2 and 3 suggest that WAM produces a more realistic Hs and Tc variability than WWIII. The different performances of the model in the Atlantic Ocean and Bay of Bengal are solely dependent on the model physics, numerics, model grid resolution and quality of wind

3.1. Significant wave height (Hs in m)				
WAM/WWIII				
S. No.	Statistical estimates	Bay of Bengal		
		BD08	BD11	BD14
1	Mean (Buoy)	2.1	1.9	2.9
2	Range (Buoy)	1.3–3.1	1.4–2.8	2.0–3.8
3	Mean (WAM/WWIII)	1.8/1.7	2.0/1.8	2.4/2.3
4	Range (WAM/WWIII)	1.3–2.4/1.2–2.3	1.3–2.7/1.3–2.5	1.7–2.9/1.7–2.8
5	R	0.93/0.95	0.95/0.94	0.96/0.97
6	SI	0.06/0.09	0.01/0.02	0.10/0.13
7	B	0.31/0.40	0.11/0.14	0.49/0.57
8	RMSE	0.13/0.19	0.03/0.03	0.30/0.38
9	PE	17.8/23.8	8.5/9.1	20.2/24.1
10	MPI	0.94/0.91	0.98/0.98	0.92/0.87
3.2. Mean wave period (Tc in s)				
WAM/WWIII				
1	Mean (Buoy)	6.2	5.9	6.8
2	Range (Buoy)	5.3–7.8	4.9–7.1	6.0–7.6
3	Mean (WAM/WWIII)	5.8/5.6	6.0/5.9	6.4/6.6
4	Range (WAM/WWIII)	4.9–6.8/4.8–6.7	5.2–6.7/5.3–6.6	5.8–6.8/6.0–7.0
5	R	0.94/0.93	0.71/0.68	0.82/0.53
6	SI	0.04/0.06	0.02/0.02	0.02/0.02
7	B	0.41/0.59	-0.05/-0.04	0.20/-0.07
8	RMSE	0.23/0.40	0.12/0.11	0.10/0.10
9	PE	7.3/10.3	4.5/4.1	4.2/3.9
10	MPI	0.96/0.94	0.98/0.98	0.98/0.98

R: Correlation Coefficient; SI: Scatter Index; B: Bias; RMSE: Root Mean Square Error; PE: Percentage Error; MPI: Model Performance Index

Table 3: Statistics of the comparison between WAM/WWIII model wave parameters and buoy measurements in the North Indian Ocean (Bay of Bengal) during July 2011.

inputs. A potential source of error in the performances of the models is the parameterization of atmospheric drag in the wind input source term. The remaining source terms such as wave wave interaction and dissipation also have considerable influences in the performance of WAM and WWIII. The wave wave interaction term used the Discrete Interaction Approximation (DIA) of Hasselmann and Hasselmann [20]; in which; away from the spectral peak and in multimodal wave fields the DIA greatly under samples the complex set of nonlinear interactions [21] leading to erroneous estimates of spectral source function, which will potentially result in shapes, deviating from observations. Apart from this, most importantly in both the models, the different representation of swell propagation in model physics could be a possible reason for deviations at the buoy location.

Summary and Conclusion

In this study, the state of the art wave models WAM and WWIII were utilized to hindcast waves using OSCAT winds for a one year period (January to December 2011) over the globe and in the North Indian Ocean (Bay of Bengal). The models implemented for the globe (77°S to 77°N and 0° to 360°E) over 1° × 1° resolution was found suitable to provide boundary inputs to the regional model domain (0°N to 30°N, 50°E to 100°E, North Indian Ocean). The WAM and WWIII model hindcasted wave parameters were validated against a selected NDBC buoy in the North Atlantic Ocean and the available NIOT buoy measurements (BD08, BD11, and BD14) in the North Indian

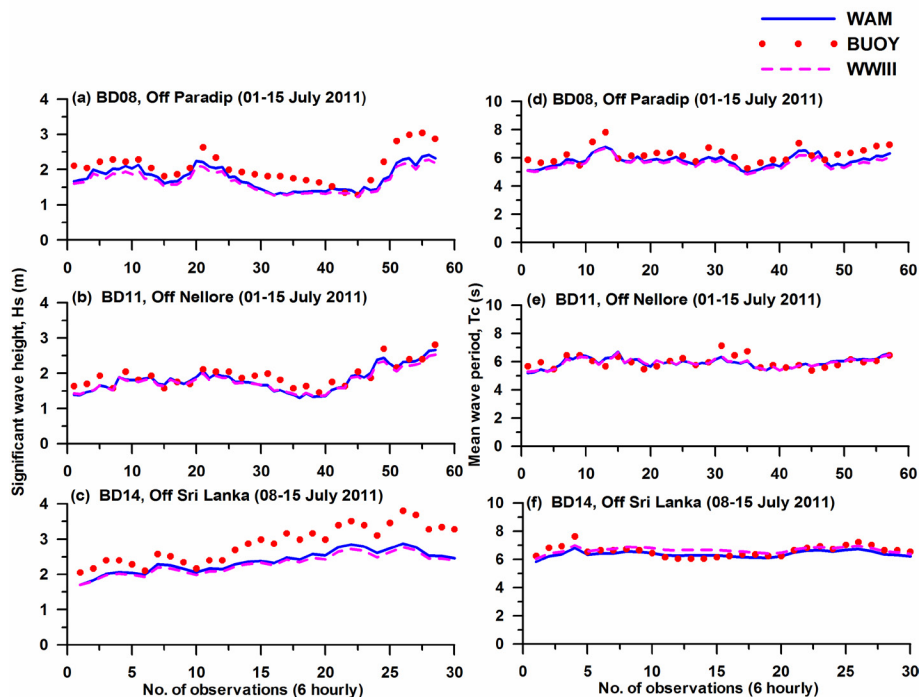


Figure 8: Comparisons between the observed (NIOT buoy) and WAM/ WWIII predicted wave parameters at 6 hourly intervals for the period 1-15 July 2011, and using OSCAT winds.

Ocean (Bay of Bengal). The spatial distributions of H_s , T_c , H_{sw} , and mean wave direction over the North Indian Ocean based on WAM and WWIII hindcasts using OSCAT winds alone appeared realistic when the wave fields were compared with each other. In this study, the model performances of WAM and WWIII were evaluated through an extensive and robust statistical error analysis. Overall, both models achieve relatively high skill in their ability to simulate H_s and T_c at the buoy locations considered in this study.

The quality of OSCAT derived winds was evaluated by validating the OSCAT retrieved wind vectors over the global ocean with *in situ* wind measurements from NDBC. The comparison of OSCAT winds with data from moored buoys indicates the RMSE of 1.18 m/s in wind speed for the speed range 4 to 24 m/s. Hindcast time series of wave heights at selected buoy locations in the Atlantic Ocean and Bay of Bengal indicate that, WAM represents the maximum and minimum wave heights much more realistically than WWIII (Figures 7 and 8). Although the correlation coefficients and MPI are systematically better for WWIII; the RMSE, SI and PE are higher in all cases with significant underestimations at the buoy locations considered in this study. Differences in the statistical analysis of wave parameters between both models are moderate. The statistical results reported in Table 2 and 3 suggest that WAM performs better than WWIII, in comparison with the observed H_s and T_c wave data. In the North Atlantic Ocean, WAM appears to behave significantly better than WWIII, based on the PE (<16% for H_s and <9% for T_c). The validations of WAM and WWIII models using NIOT buoy measurements in the Bay of Bengal indicate that during the month of July 2011, the performance of WAM was relatively better than WWIII. The observed and predicted wave parameters of WAM and WWIII show percentage error ranging from 9 to 24% for H_s and within 10% for T_c . The percentage error from WWIII model as compared to WAM was higher for H_s by 1-6%. In

addition, it is higher by 1-3% in case of T_c . Hence, the study reveals that, during July 2011 (south-west monsoon season) the performance of both WAM and WWIII models are in good agreement with each other. Many factors such as quality of input winds swell propagation in model physics, model grid resolution can contribute to significant departures in the performances in the models. The study further suggests that, a long-term wave hindcast database for the North Indian Ocean region can bring out further confidence with suitable validations using available wave measurements. The long-term predicted/simulated fields will be very useful for most of the user community dealing with various coastal/offshore activities and for defence applications besides the research and developmental needs.

Acknowledgement

The authors express their sincere thanks to Director, NPOL, Group Head, Ocean Science Group of NPOL for their encouragement and facilities provided to carry out this work. This is a part of the Ph.D. work of Umesh P. A., carried out under a collaborative project between NPOL and SAC, Ahmedabad (Project: NPOL/SAC-II) at Naval Physical and Oceanographic Laboratory, DRDO, Cochin. The authors express their sincere thanks to Director, SAC and Director, NRSC for providing the required wind data used for execution of the wave model. They are also grateful to Director, NIOT (National Institute of Technology, Chennai) and Director, INCOIS (Indian National Centre for Ocean Information Services, Hyderabad) who have provided wave data for this study.

References

1. WAMDI Group (1988) The WAM model- A third generation ocean wave prediction model. J Phys Oceanogr 18: 1775-1810.
2. Prasad KB, Kalra R, Dube SK, Sinha PC, Rao AD (2004) Sea State Hindcast with ECMWF data using a Spectral wave model for typical monsoon months. Nat Hazards 31: 537-548.
3. Vethamony P, Sudheesh K, Rupali SP, Babu MT, Jayakumar S, et al. (2006) Wave modelling for the North Indian Ocean using MSMR analysed winds. Int J Rem Sens 27: 3767-3780.

4. Remya PG, Kumar R, Basu S, Sarkar A (2012) Wave hindcast experiments in the Indian Ocean using MIKE21 SW model. *J Earth Syst Sci* 121: 385-392.
5. Nayak S, Bhaskaran PK, Venkatesan R, Dasgupta S (2013) Modulation of local wind waves at Kalpakkam from remote forcing effects of Southern Ocean swells. *Ocean Eng* 64: 23-35.
6. Sandhya KG, Balakrishnan Nair TM, Bhaskaran PK, Sabique L, Arun N, et al. (2014) Wave forecasting system for operational use and its validation at coastal Puducherry, east coast of India. *Ocean Eng* 80: 64-72.
7. Samiksha SV, Polnikov VG, Vethamony P, Rashmi R, Pogarskii F, et al. (2015) Verification of model wave heights with long term moored buoy data: Application to wave field over the Indian Ocean. *Ocean Eng* 104: 469-479.
8. Amrutha MM, Sanil Kumar V, Sandhya KG, Balakrishnan Nair TM, Rathod JL (2016) Wave hindcast studies using SWAN nested in WAVEWATCH III-comparison with measured nearshore buoy data off Karwar, eastern Arabian Sea. *Ocean Eng* 119: 114-124.
9. Umesh PA, Bhaskaran PK, Sandhya KG, Balakrishnan Nair TM (2017) An assessment on the impact of wind forcing on simulation and validation of wave spectra at coastal Puducherry, east coast of India. *Ocean Eng* 139: 14-32.
10. Tolman HL (2009) User Manual and system documentation of WAVEWATCH III™ Version 3.14. NOAA/NWS/NCEP/MMAB Technical Note 276, 220.
11. Tolman HL, Chalikov DV (1996) Source terms in a third-generation wind-wave model. *J Phys Oceanogr* 26: 2497-2518.
12. Gunther H, Behrens A (2011) The WAM model-validation document version 4.5.3.; Helmholtz-Zentrum Geesthacht (HZG), Centre for Materials and Coastal Research, Teltow.
13. Swain J, Umesh PA (2013) Global analysis of OSCAT winds for sea-state prediction using third generation wave models. In: Baba M and Jayachandran KV (eds.) Proceedings of National Conference of Ocean Society of India (OSICON 2013), Role of Oceans in Earth System, IITM, Pune pp: 24-28.
14. Bonjean F, Lagerloef GSE (2002) Diagnostic model and analysis of the surface currents in the Tropical Pacific Ocean. *J Phys Oceanogr* 32: 2938-2954.
15. Padilla-Hernandez R, Perrie W, Toulany B, Smith PC (2007) Modeling of two northwest Atlantic storms with third-generation wave models. *Wea Forecasting* 22: 1229-1242.
16. Bhowmick SA, Ruchi M, Sandhya KG, Seemanth M, Nair TMB, et al. (2015) Analysis of SARAL/AltiKa wind and wave over Indian Ocean and its real-time application in wave forecasting system at ISRO. *Mar Geod* 38: 396-408.
17. Kumar R, Abhisek C, Anant P, Rajesh S, Bhawani SG, et al. (2013) Evaluation of Oceansat-2 derived ocean surface winds using observations from global buoys and other Scatterometer IEEE Transac on Geosci Rem Sens 51: 2571-2576.
18. Hastenrath S, Lamb PJ (1979) Climatic atlas of the Indian Ocean, Part-I: Surface climate and atmospheric circulation. The University of Wisconsin Press, USA p: 117.
19. Bigg GR (1996) Atlas of the oceans: Wind and wave climate. In: Young IR and Holland GJ (eds.) Pergamon, Elsevier Science Ltd., NY, USA pp: xvi+241.
20. Hasselmann K, Hasselmann S (1985) The wave model EXACT-NL, In: The SWAMP Group (ed.) Ocean Wave Modelling, Plenum Press. New York and London p: 256.
21. Hanson JL, Tracy BA, Tolman HL, Scott RD (2009) Pacific hindcast performance of three numerical wave models. *J Atmos Oceanic Technol* 26: 1614-1633.